

Interacting Electron Theory of Coherent Nonlinear Response

M. Z. Maialle and L. J. Sham

Department of Physics, University of California, San Diego, La Jolla, California 92093-0319

(Received 11 July 1994)

A theory of the nonlinear susceptibility for a two-band semiconductor model is given as a perturbation series in the external oscillating electric field and in the carrier interaction. Diagrammatic representation makes clear both the structure of subsets of the perturbation series for resummation and the corresponding physical processes. The theory, applied to four-wave mixing in quantum wells, provides a unified basis for understanding a wide range of observed phenomena.

PACS numbers: 78.47.+p, 42.50.Md, 71.35.+z, 78.66.-w

A number of four-wave mixing (FWM) experiments [1,2] have shown that there are effects of the many-body interaction on the nonlinear optical process which cannot be explained by only the excitons in a two-level-system model [3]. Some of the observed interaction effects have been explained in terms of the self-energy and local-field corrections [4,5]. For phenomena which involve polarization dependence [6–8], the recently proposed explanations [9–11] invoke the existence of a biexciton state. In this Letter, we present a brief, physical account of a unified theory of the nonlinear response, from which all such effects as the local-field effects and biexcitons can be derived. Thus, the theory provides the first-principles origin of these interaction effects, including the parameters which govern their behavior as well as a physical picture of what the effects are, thereby giving a perspective of their relationship. This single theory is used to provide an explanation for all the diverse observations in FWM, including the rise of the FWM signal for negative delay time, the difference between copolarization and cross polarization, and quantum beatings of the photon echo.

Such a theory is possible because it is a perturbation theory of the induced polarization to a given order of the electric field of the light wave (e.g., the third-order susceptibility χ_3 for FWM). This provides a limitation on the possible ways in which the interaction enters. This was first exploited by Axt and Stahl [12] by an equation of motion method of the density matrices to factorize the n -point density matrices to a required order of the electric field and, thus, to decouple the equations of motion exactly to that order of the electric field. We have developed a diagrammatic method of the perturbation series in the electric field and in the interaction effects. We take the opposite tack of starting with the noninteracting susceptibility of a given order in the electric field and then decorate the diagram with interaction lines. The diagrams make it transparent what interaction processes are present to a given order of the electric field. In χ_3 for FWM, the diagram shows two incoming excitons and two outgoing ones. From the possible interaction diagrams of the two excitons, we can easily discern the local-field effect, the biexciton,

and the two excitons with different spins producing polarization effects.

Figure 1(a) shows the third-order susceptibility χ_3 as a four-point vertex diagram. With the time axis pointing vertically up, the diagram represents the mixing of waves of wave vector \mathbf{k}_1 , \mathbf{k}_2 , and \mathbf{k}_3 to yield a signal at $\mathbf{k}_f = -\mathbf{k}_1 + \mathbf{k}_2 + \mathbf{k}_3$. In the two-pulse FWM, \mathbf{k}_2 and \mathbf{k}_3 are taken to be from the same wave. In that case, the delay time T is the time between the two external pulses \mathbf{k}_2 and \mathbf{k}_1 .

To simplify the description of the near-resonant excitation in a semiconductor quantum well, we consider a two-band model with a ground state of an empty conduction subband and a full valence subband. A conduction electron carries a wave vector \mathbf{k} and spin $\sigma = \pm\frac{1}{2}$ and a heavy valence hole wave vector $-\mathbf{k}$ and spin $m = \pm\frac{3}{2}$. The perturbation term of the Hamiltonian includes the interaction with the laser's electric field \mathcal{E}_s with circular

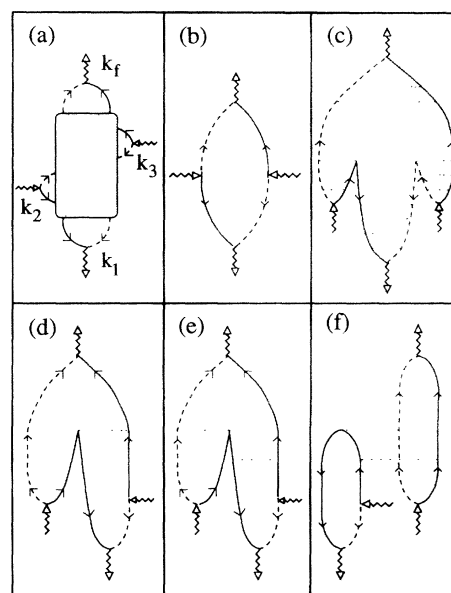


FIG. 1. Diagrammatic representation for the χ_3 processes. For explanation, see text.

polarization $s = \pm 1$, associated with the dipole moment μ_{som} , permitting the vertical transition conserving angular momentum $s = m + \sigma$. The perturbation also contains the Coulomb interaction between two carriers, conduction electron or valence hole [4]. Neglected are the exchange interaction [13] between an electron and a hole and the interband excitation of an electron-hole pair. The effect of the latter is included by the dielectric constant in the Coulomb interaction.

The simplest diagram for χ_3 is one without any Coulomb interaction [Fig. 1(b)], showing a loop with the solid segment representing a conduction electron propagator and the broken line a valence hole, with the time axis vertically up. The energy conservation of a wave exciting an electron-hole pair, or the reverse, at each vertex gives the "rotating-wave approximation" [14]. The angular momentum conservation at each vertex yields the polarization dependence of the light wave. Diagram rules, similar to those in the field theory, will be given in a longer paper. Evaluation of this diagram corresponds exactly to the expression given by Ref. [3]. Since a loop with a reversed time order of \mathcal{E}_1 and \mathcal{E}_2 would violate the exclusion principle, no negative time-delay signal is predicted for a noninteracting system [3].

To include the Coulomb interaction in the susceptibility, we decorate the four-point vertex with horizontal dotted Coulomb interaction lines with the following rules: (1) An electron or hole line may create in the decreasing time direction a pair of lines of the same band with arrows in opposite time directions and (2) two parallel lines may be joined by an interaction line only if their arrows point in the same direction.

An interaction line across each vertex forms the first term of a ladder sum of repeated attraction between a hole and an electron propagating in the same direction, as shown in Fig. 1(c), which includes the local-field effect [4,5]. Summation of these ladders produces exciton binding. Thus, the most basic process in FWM is the production of two excitons which, without further interaction, change their partners to produce two new excitons.

The remaining possibilities of decorating Fig. 1(b) with one Coulomb line is to join the two electron or hole lines on opposite sides, as shown by Fig. 1(d). For clarity, we have not drawn the lines across each vertex for the excitons. This first-order interaction between two excitons coincides with the so-called self-energy correction [4,5]. It is also evident that the time order of the two pulses \mathcal{E}_1 and \mathcal{E}_2 can now be reversed in Figs. 1(c) and 1(d) and in the rest of the terms involving interaction.

By rule (2), the interaction lines joining two excitons propagating in the same time direction, such as those produced by \mathcal{E}_2 and \mathcal{E}_3 , can cause the two excitons to form a biexciton. By the same rule, there is no interaction between the biexciton and the exciton line going in the opposite time direction.

The FWM diagram, Fig. 1(a), shows four external field lines, two going in and two out. Since, by energy conservation, each closed fermion loop must contain an equal number of ingress and egress lines, the maximum possible number of loops for a four-vertex diagram is two. Figures 1(e) and 1(f) are two examples of one-loop and two-loop terms of the same order in interaction. In a single loop, from the angular momentum conservation, all the four electric field lines must be of the same circular polarization s , all the electron and hole lines must have the same σ and m with $s = \sigma + m$. On the other hand, in the two-loop diagram, the polarization in one loop may be the same as or different from the other loop. To first order in the interaction, only one loop is possible, leading to interaction between two excitons of the same spin. The first-order interaction connecting two loops would have zero momentum, leading to a zero interaction matrix element. Thus, the local-field effect alone contains no polarization mixing. To second and higher orders in the interaction, the interaction between two excitons of the same spin comes from both one- and two-loop diagrams, whereas the interaction between two excitons of opposite spins comes only from two-loop diagrams. In a two-pulse FWM experiment, the third-order polarization has circular components of the form

$$P_s^{(3)} = \sum_{s'} \chi_{ss'} \mathcal{E}_{1s'}^* \mathcal{E}_{2s'} \mathcal{E}_{2s}, \quad (1)$$

where the third-order susceptibility χ_{++} is the sum of all one-loop and two-loop diagrams with $s = 1$ polarizations, and χ_{+-} the sum of two-loop diagrams only with two pairs of opposite polarizations. If the electric fields are linearly polarized with \mathcal{E}_1 at an angle φ to \mathcal{E}_2 along the x direction, then

$$\begin{aligned} P_x^{(3)} &= (\chi_{++} + \chi_{+-}) \mathcal{E}_1 \mathcal{E}_2^2 \cos \varphi, \\ P_y^{(3)} &= (\chi_{++} - \chi_{+-}) \mathcal{E}_1 \mathcal{E}_2^2 \sin \varphi. \end{aligned} \quad (2)$$

The existence of the two-loop diagrams is necessary for the polarization difference which has been observed [6,11].

The net result of the diagrammatic analysis is that the four-point vertex function can be expressed in terms of the exciton and the biexciton. To obtain an approximate expression for the FWM signal in the coherent limit [12], exciton and biexciton states are assumed to have been evaluated, and a phenomenological relaxation time is added to each exciton (γ_2^x) or biexciton (γ_2^{xx}) propagator. Then, approximately,

$$\chi_{ss'} = (X_s + Y_{ss}) \delta_{ss'} + Y_{ss'}. \quad (3)$$

The one-exciton contribution is given by

$$X_s = \kappa \sum_{\alpha} e^{-\gamma_2^x t - i\nu_{s\alpha}(t-2T)} \Theta(T) \Theta(t-T) \phi_{s\alpha}^2, \quad (4)$$

where $\kappa = -i|\mu|^4/\hbar^3$, $\nu_{s\alpha}$ is the exciton energy difference from the light frequency, and $\phi_{s\alpha}$ the exciton wave function at zero relative distance. The biexciton contribution is given by

$$Y_{ss'} = \kappa \sum_{\alpha\alpha'\lambda} \phi_{s\alpha} e^{-\gamma_2^x t - i\nu_{s\alpha}(t-2T)} \frac{\Delta_{ss'\lambda}^{s\alpha, s'\alpha'}}{\Delta_{ss'\lambda}^{s\alpha, s'\alpha'} + i\gamma_2^{xx}} T_{ss'\lambda}^{s\alpha, s'\alpha'} [\Theta(T)\Theta(t-T)e^{-i(\nu_{s\alpha} - \nu_{s'\alpha'})T} (1 - e^{(i\Delta_{ss'\lambda}^{s\alpha, s'\alpha'} - \gamma_2^{xx})(t-T)}) + \Theta(-T)\Theta(t)e^{-[i(2\nu_{s\alpha} - \Omega_{ss'\lambda}) - \gamma_2^{xx}]T} (1 - e^{(i\Delta_{ss'\lambda}^{s\alpha, s'\alpha'} - \gamma_2^{xx})t})], \quad (5)$$

where $\hbar\Delta_{ss'\lambda}^{s\alpha, s'\alpha'}$ is the binding energy of the biexciton in state $ss'\lambda$, and $\hbar\Omega_{ss'\lambda}$ is the difference between the biexciton energy and the two-photon transition energy. The transition matrix element connecting the biexciton state $ss'\lambda$ to two excitons $s\alpha$ and $s'\alpha'$ and to the \mathcal{E}_2 photons times $\phi_{s'\alpha'}$ is denoted by $T_{ss'\lambda}^{s\alpha, s'\alpha'}$.

Consider the case where the biexciton binding Δ is much stronger than the biexciton dephasing rate γ_2^{xx} . We further confine the exciton to a single state. Then the third-order susceptibilities reduce to

$$X_s = \kappa e^{-\gamma_2^x t - i\nu_s(t-2T)} \phi_s^2 \Theta(T)\Theta(t-T), \quad (6)$$

$$Y_{ss'} = \kappa e^{-\gamma_2^x t - i\nu_s(t-2T)} \phi_s \phi_{s'} \left\{ \Theta(T)\Theta(t-T) \left[1 - \sum_{\lambda} |M_{ss'\lambda}(\lambda)|^2 e^{(i\Delta_{ss'\lambda} - \gamma_2^{xx})(t-T)} \right] + \Theta(-T)\Theta(t) \sum_{\lambda} e^{-i(\Delta_{ss'\lambda} - \gamma_2^{xx})T} |M_{ss'\lambda}(\lambda)|^2 (1 - e^{(i\Delta_{ss'\lambda} - \gamma_2^{xx})t}) \right\}, \quad (7)$$

where $M_{ss'}$ represents the simplified exciton-biexciton transition matrix. Equation (7) is similar to the result derived from a multilevel system including a biexciton [9].

This limit of large Δ corresponds to the case where the biexciton state is important for the nonlinear optical process as observed in several recent experiments [9,10,15]. In particular, Wang *et al.* [11] have measured a biexciton binding energy of 1.2 meV (or $\Delta \approx 1.8$ ps⁻¹) and a corresponding dephasing rate of $\gamma_2^{xx} \approx 0.5$ ps⁻¹, within the limit discussed here. In the opposite, weak biexciton binding limit, where $\Delta \ll \gamma_2^{xx}$, Eq. (3) reduces to the one derived by Wegener *et al.* [5] using the Hartree-Fock (HF) modified semiconductor Bloch equations (SBE) with the local-field effects.

In two-pulse FWM experiments performed with linearly polarized light [1,6,7], the self-diffracted signal is observed to be much stronger in copolarization than in cross polarization [7,8]. The HF solution of the SBE is unable to explain such an effect but Eq. (3) can, as can a multilevel model including a biexciton [9,10], which is equivalent to a further approximation to Eq. (7) that two excitons with parallel spins have negligible binding energy (i.e., $\Delta = 0$ for $s = s'$), retaining only biexcitons with antiparallel-spin excitons. The result for $T > 0$ is

$$\begin{aligned} \begin{bmatrix} P_x^{(3)}(t) \\ P_y^{(3)}(t) \end{bmatrix} &\propto e^{-\gamma_2^x t} \Theta(t-T) \begin{bmatrix} \cos \varphi \\ \sin \varphi \end{bmatrix} \left\{ \begin{bmatrix} 2 \\ 0 \end{bmatrix} e^{-i\nu(t-2T)} \right. \\ &\left. - |Ms\bar{s}|^2 e^{i\nu t - (i\Omega + \gamma_2^{xx})(t-T)} \right\}. \quad (8) \end{aligned}$$

Since $|Ms\bar{s}| \leq 1$, the copolarized excitation ($\varphi = 0$) is stronger than the cross-polarized excitation ($\varphi = \pi/2$).

Another important observation is the photon-echo behavior of the copolarized signal, in contrast to the simple decay exhibited by the cross-polarized one [1,6]. For

inhomogeneously broadened systems, the total polarization is given as a sum over distributions of excitonic detuning energy ν and biexcitonic detuning energy Ω . The first term in Eq. (8), when integrated over the detunings, gives rise to a photon echo at $t = 2T$. The second term appears as a product of distributions centered at $t = 0$ (due to the integration over ν) and $t = T$ (due to Ω). Therefore, this result shows that only the copolarized signal ($\varphi = 0$) can exhibit a photon echo. The cross-polarized signal shows a more complicated decay than that described by γ_2^x [3]. In a nonmagnetic system, if the difference due to phase space filling is unimportant, the two-loop contributions of χ_{++} and χ_{+-} cancel in $P_y^{(3)}$ of Eq. (2), which is then dominated by the parallel-spin biexciton. This would contradict the antiparallel-spin biexciton model [9,10] in which, as in Eq. (8), $P_y^{(3)}$ is determined by the antiparallel-spin biexciton.

Recent FWM measurements in a quantum well [16] have shown that the excitation of two inhomogeneously broadened exciton transitions of different energies leads to a photon echo with quantum beatings. The cause was inferred to be the coupling of two excitons in islands of thickness differing by one monolayer [17]. We suggest that the observed oscillations on the echo amplitude may be caused by a biexciton state formed by excitons in different islands. The theory has the same form as above, except the polarization index s now represents an island of a particular thickness. The coupling between two excitons is the same as the interaction terms in the two-loop diagrams. The exciton energy distribution is taken to be bimodal with a mean separation $\hbar 2D_{ss'}$ for $s \neq s'$, equal to the energy difference of the two excitons belonging to islands differing by one monolayer thickness. Then, the FWM signal has an oscillatory term $\cos(D_{ss'} 2T)$ in the echo amplitude.

In summary, we have given a brief description of a unified theory of the nonlinear polarizability in a quantum well. The diagrammatic representation provides both a quantitative theory and a physical picture for a wide range of observed phenomena in the two-pulse FWM experiments. The role of the interaction in providing the rise in negative delay time is evident. The difference between the interaction for two excitons of the same or opposite spins leads to a simple physical explanation of the polarization mixing. The same physics applied to a distribution of exciton energies also gives an explanation of the photon-echo-amplitude oscillations in a quantum well with islands. In the applications of our theory, we have concentrated on the coherence regime and treated the relaxation processes in the relaxation time approximation. In future work, we plan to use our theory to investigate dephasing and relaxation [18].

We thank D.G. Steel and Th. Östreich for helpful discussions. This research was supported in part by NSF Grant No. DMR 91-17298. M.Z.M. acknowledges a fellowship from CNPq, Brazil.

-
- [1] D. S. Kim, J. Shah, T. C. Damen, W. Schäfer, F. Janhnke, S. Schmitt-Rink, and K. Köhler, *Phys. Rev. Lett.* **69**, 2725 (1992).
 - [2] S. Weiss, M. A. Mycek, J. Y. Bigot, S. Schmitt-Rink, and D. S. Chemla, *Phys. Rev. Lett.* **69**, 2685 (1992).
 - [3] T. Yajima and Y. Taira, *J. Phys. Soc. Jpn.* **47**, 1620 (1990).
 - [4] M. Lindberg and S. W. Koch, *Phys. Rev. B* **38**, 3342 (1988).
 - [5] M. Wegener, D. S. Chemla, S. Schmitt-Rink, and W. Schäfer, *Phys. Rev. B* **42**, 5675 (1990).
 - [6] S. T. Cundiff, H. Wang, and D. G. Steel, *Phys. Rev. B* **46**, 7248 (1992).
 - [7] D. Bennhardt, P. Thomas, R. Eccleston, E. J. Mayer, and J. Kuhl, *Phys. Rev. B* **47**, 13 485 (1993).
 - [8] S. Schmitt-Rink, D. Bennhardt, V. Heuckeroth, P. Thomas, P. Haring, G. Maidorn, H. Bakker, K. Leo, D. S. Kim, J. Shah, and K. Köhler, *Phys. Rev. B* **46**, 10460 (1992).
 - [9] K. Bott, O. Heller, D. Bennhardt, S. T. Cundiff, P. Thomas, E. J. Mayer, G. O. Smith, R. Eccleston, J. Kuhl, and K. Ploog, *Phys. Rev. B* **48**, 17 418 (1993).
 - [10] T. Saiki, M. Kuwata-Gonokami, T. Matsusue, and H. Sakaki, *Phys. Rev. B* **49**, 7817 (1994).
 - [11] H. Wang, J. Shah, T. C. Damen, and L. N. Pfeiffer (to be published).
 - [12] V. M. Axt and A. Stahl, *Z. Phys. B* **93**, 195 (1994); **93**, 205 (1994).
 - [13] A. Stahl, *Z. Phys. B* **72**, 371 (1988); M. Z. Maialle, E. A. de Andrada e Silva, and L. J. Sham, *Phys. Rev. B* **47**, 15 776 (1993).
 - [14] L. Allen and J. H. Eberly, *Optical Resonance and Two-Level Atoms* (Dover, New York, 1987), p. 41.
 - [15] G. Finkelstein, S. Bar-Ad, O. Carmel, and I. Bar-Joseph, *Phys. Rev. B* **47**, 12 964 (1993).
 - [16] M. Koch, J. Feldmann, E. O. Göbel, P. Thomas, J. Shah, and K. Köhler, *Phys. Rev. B* **48**, 11 480 (1993).
 - [17] M. Koch, J. Feldmann, G. von Plessen, E. O. Göbel, P. Thomas, and K. Köhler, *Phys. Rev. Lett.* **69**, 3631 (1992).
 - [18] T. Rappen, U. G. Peter, M. Wegener, and W. Schäfer, *Phys. Rev. B* **49**, 10 774 (1994).

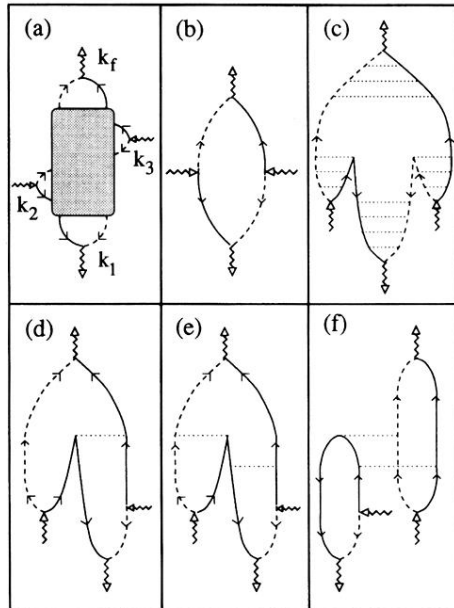


FIG. 1. Diagrammatic representation for the χ_3 processes. For explanation, see text.